

# Radiocarbon Analysis of Individual Amino Acids: Carbon Blank Quantification for a Small-Sample High-Pressure Liquid Chromatography Purification Method

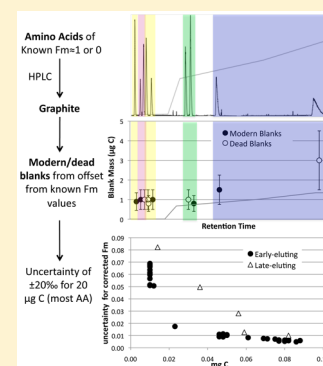
Amy L. Bour,<sup>\*,†</sup> Brett D. Walker,<sup>‡</sup> Taylor A. B. Broek,<sup>†</sup> and Matthew D. McCarthy<sup>\*,†</sup>

<sup>†</sup>Ocean Sciences Department, University of California, Santa Cruz, 1156 High Street, Santa Cruz, California 95064, United States

<sup>‡</sup>Keck Carbon Cycle AMS Laboratory, University of California, Irvine, 2212 Croul Hall, Irvine, California 92697, United States

## S Supporting Information

**ABSTRACT:** Compound-specific radiocarbon analysis (CSRA) of amino acids (AAs) is of great interest as a proxy for organic nitrogen (N) cycling rates, dating archeological bone collagen, and investigating processes shaping the biogeochemistry of global N reservoirs. However, recoverable quantities of individual compounds from natural samples are often insufficient for radiocarbon ( $^{14}\text{C}$ ) analyses ( $<50\ \mu\text{g C}$ ). Constraining procedural carbon (C) blanks and their isotopic contributions is critical for reporting of accurate CSRA measurements. Here, we report the first detailed quantification of C blanks (including sources, magnitudes, and variability) for a high-pressure liquid chromatography (HPLC) method designed to purify individual AAs from natural samples. We used pairs of AA standards with either modern (M) or dead (D) fraction modern (Fm) values to quantify MC and DC blanks within several chromatographic regions. Blanks were determined for both individual and mixed AA standard injections with peak loadings ranging from 10 to 85  $\mu\text{g C}$ . We found  $0.8 \pm 0.4\ \mu\text{g}$  of MC and  $1.0 \pm 0.5\ \mu\text{g}$  of DC were introduced by downstream sample preparation (drying, combustion, and graphitization), which accounted for essentially the entire procedural blank for early eluting AAs. For late-eluting AAs, higher eluent organic content and fraction collected volumes contributed to total blanks of  $1.5 \pm 0.75\ \mu\text{g}$  of MC and  $3.0 \pm 1.5\ \mu\text{g}$  of DC. Our final measurement uncertainty for 20  $\mu\text{g}$  of C of most AAs was  $\pm 0.02\ \text{Fm}$ , although sample size requirements are larger for similar uncertainty in late-eluting AAs. These results demonstrate the first CSRA protocol for many protein AAs with uncertainties comparable to the lowest achieved in prior studies.



The development of radiocarbon ( $^{14}\text{C}$ ) dating using accelerator mass spectrometry (AMS) initiated a renaissance for this measurement by drastically decreasing sample size and measurement time requirements.<sup>1</sup> AMS made  $^{14}\text{C}$  measurements possible in a wide range of new sample-limited studies, including many that focus on cycling of diffuse environmental carbon (C) reservoirs. However, the myriad processes shaping bulk  $^{14}\text{C}$  content of environmental organic samples still pose a major problem in interpretation of a given sample's age.<sup>2</sup> As AMS sample size requirements have continued to decrease, compound-specific radiocarbon analysis (CSRA) of biomarker molecules has emerged as a way to bypass this challenge.<sup>3,4</sup> CSRA now has many environmental applications, which have become invaluable in understanding transformations and exchanges between C reservoirs on earth. For example, CSRA of membrane lipids has allowed quantification of ocean archaeal chemoautotrophy,<sup>5</sup> revealed organic C substrate preferences of soil bacterial groups,<sup>6</sup> and elucidated mechanisms for remediation of petroleum-impacted soils.<sup>7</sup> CSRA has been applied to DNA as a way to determine the C sources for various marine microbial communities.<sup>8,9</sup> CSRA of alkenones has also improved paleotemperature reconstructions.<sup>10</sup> Finally, CSRA of lignin allows for tracking higher-plant-derived terrestrial organic C.<sup>11,12</sup>

CSRA of amino acids (CSRA-AA) holds enormous potential across a wide range of disciplines. Amino acids (AAs) represent a major fraction of all cellular C and nitrogen (N). AAs are also present in all detrital organic matter and represent the main isolable form of organic N that cycles in natural waters, soils, and sediments.<sup>13</sup> AA distributions, C- and N-stable isotope ratios, and chirality comprise a powerful set of tracers for multiple environmental processes.<sup>14–18</sup> Natural abundance CSRA-AA could add a  $^{14}\text{C}$  “clock” and isotopic source endmember to the information potential of individual AAs; however, this approach is in its infancy. Current CSRA-AA data is restricted to archeological studies focused on a single AA (hydroxyproline), which serves as a biomarker to allow more accurate dating of bone collagen samples independent of burial or preservation effects.<sup>19,20</sup> However, more routine CSRA-AA methods capable of providing  $^{14}\text{C}$  information across a wider range of naturally occurring AAs would represent an extremely powerful tool for investigating the age and cycling of organic N across many scientific disciplines.

Received: September 23, 2015

Accepted: February 8, 2016

Such new CSRA-AA methods would require isolation methods for a broader suite of individual AAs derived from complex environmental matrices. Purifications of lipid biomarkers from sediments<sup>21</sup> and lignin-derived phenols from wood<sup>12</sup> for CSRA have previously been achieved using preparative capillary gas chromatography (PCGC). However, PCGC often requires quantitative C addition during the derivatization of target compounds, increasing C blanks. For avoiding this added derivative C, more recent CSRA studies of biomarkers have instead utilized high performance liquid chromatography (HPLC).<sup>11,22</sup> The use of HPLC also reduces the number of injections needed to purify an adequate amount of material<sup>11</sup> and has no potential for sample loss due to trapping inefficiencies.<sup>23</sup> However, HPLC approaches do introduce a chromatography blank.

AMS <sup>14</sup>C values always represent a mixture of target molecule C and procedural blank C (exogenous C). Therefore, quantification of both the magnitude and the isotopic composition of the exogenous C blank is critical for any CSRA approach. Depending on the isotopic offset between the target compound and exogenous C, even a small amount of contamination can drastically alter the accuracy of measured <sup>14</sup>C fraction modern (Fm) results, especially for small samples. In HPLC methods, potential exogenous C sources include both stationary and mobile phases, such that the isolation protocol can contribute significantly to the final <sup>14</sup>C Fm values.<sup>22,24</sup> The mass and Fm of procedural C blanks have previously been quantified for HPLC purifications of lipids and lignin phenols from environmental matrices<sup>11,22</sup> and for the isolation of hydroxyproline from bone collagen.<sup>19</sup> Although several HPLC methods have been developed to quantify<sup>25,26</sup> or purify underivatized AA for stable isotopic analysis,<sup>27,28</sup> to our knowledge no prior study has presented a method for a full AA suite with rigorously quantified <sup>14</sup>C blanks.

Here, we report the magnitude, isotopic composition, and sources of C blanks for an HPLC purification method optimized to recover individual AAs from small organic matter samples.<sup>28</sup> We conducted a series of experiments based on individual and mixed AA standards with contrasting <sup>14</sup>C content, testing the potential for coelution and elution conditions to influence sample <sup>14</sup>C Fm values. This design allowed us to simultaneously quantify both modern carbon (MC) and dead carbon (DC) endmember contributions to the total C blank for characteristic chromatographic regions. We also were able to distinguish main blank sources, focusing on levels of MC and DC contributions from column bleed, the solvent system, and peak fronting/tailing effects. We report that this method had consistently low and correctable blanks for all AAs tested, especially for the early eluting AAs. The uncertainty we report for samples as small as 20  $\mu\text{g}$  of C (1 SD <  $\pm$  0.02 Fm) represents a substantial improvement over that attainable with blank sizes reported in previous AA HPLC methods.

## EXPERIMENTAL SECTION

**Experimental Design.** Our experimental framework was designed to determine both MC and DC blank contributions to measured Fm values of purified AAs by quantifying blanks linked to HPLC eluent composition, adjacent compounds, and offline sample processing steps (Figure 1). The masses of the MC and DC blanks were determined using what is commonly referred to in <sup>14</sup>C literature as the “indirect method”, which essentially applies a standard additions approach to a series of AA standards with near-modern (Fm  $\approx$  1) or dead (Fm  $\approx$  0)

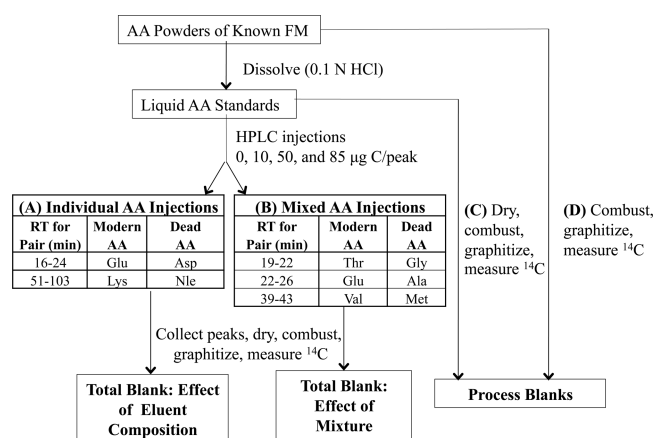


**Figure 1.** Modern and dead C contributions to the procedural blank were determined using pairs of AAs, where each pair included one AA each of known modern and dead <sup>14</sup>C composition. Blank sources were assessed by comparing results from three general treatments: (A) individual AA HPLC injections, (B) AA mixed standard HPLC injections, and (C and D) nonchromatographic process blanks. Each analysis was performed on a series of samples ranging from 10 to 85  $\mu\text{g}$  of C. For HPLC isolations, blanks were determined for pairs of standards selected to span retention times/eluent compositions.

<sup>14</sup>C composition.<sup>29</sup> Each AA standard was isolated across a range of sample sizes (10–85  $\mu\text{g}$  of C) that span reasonable sample sizes for CSRA work. Using the offsets between the measured and known AA Fm values, MC and DC blank masses were then determined by applying the indirect method to pairs of AA having similar chromatographic behavior but with contrasting <sup>14</sup>C content.<sup>24,29–31</sup> As outlined in Figure 1, our experimental design applies the same approach to AA standards processed to target blank contributions from three specific sources: (1) chromatographic elution order (changing chromatographic conditions), (2) possible coelution of adjacent peaks, and (3) offline sample processing steps (i.e., fraction collection, drying, combustion, graphitization).

The potential effects of chromatographic elution order, as a proxy for C contributions from variation in mobile phase composition, were first tested using HPLC injections of pure, single-AA standards (Figure 1A). Four standards were selected for this purpose, including one modern and one dead AA that elute early in the method (in a primarily aqueous mobile phase), and one of each that elute later (in a more organic mobile phase). With this setup, each modern/dead pair reveals the total C blank for the corresponding region of the chromatographic method. Isotopic offsets from the known Fm value of the modern AAs give the mass of the DC blank, whereas the MC blank mass is determined from the offset from the known Fm value for the dead AA standard. The total C blank for each pair of AAs is then defined as the sum of the masses of the DC and MC blanks.

Second, to investigate the potential influence of neighboring peaks having strongly contrasted <sup>14</sup>C content, standards were also injected in a mixture (Figure 1B). The AA standard mixture included three early to mideluting modern/dead pairs of AAs with the AAs within each pair eluting in close proximity to each other. The Fm values and calculated blank masses from these AAs were then compared to those from the AAs injected individually in similar chromatographic regions. Because of the extreme <sup>14</sup>C offset between dead and modern compounds, this

sensitive approach should reveal the influence of even minor peak coelutions.

Finally, we independently investigated the blank contributions from postchromatography sample processing steps (Figure 1C, D). To determine the blank associated with sample drying, liquid standards of one modern/dead AA pair having the same range of C amounts used for the HPLC tests (10–85  $\mu\text{g C}$ ) were measured directly into quartz tubes, dried, combusted, and graphitized. This test isolates the post-HPLC procedural blank from that associated with HPLC separation and fraction collection. The blank introduced during combustion (including sample amendment with combustion reagents and flame sealing) and graphitization (sealed tube zinc reduction method<sup>32,33</sup>) was determined using two dead standards and two modern standards in powder form. These were weighed directly into quartz tubes, again in the same range of sample sizes, combusted, and graphitized.

**Standard Materials.** Powdered standards of alanine (Ala), aspartic acid (Asp), glutamic acid (Glu), glycine (Gly), lysine (Lys), methionine (Met), norleucine (Nle), threonine (Thr), and valine (Val) were purchased from ACROS Organics (Morris Plains, NJ, USA), and the  $^{14}\text{C}$  isotopic content of each was measured at the W. M. Keck Carbon Cycle Accelerator Mass Spectrometry Laboratory at the University of California, Irvine (KCCAMS; Irvine, CA, USA). These measurements were performed in duplicate, using samples of 0.8 mg of C, to generate the “known values” used in this experiment with errors of  $\pm 0.0007$  Fm for dead compounds and  $\pm 0.0020$  Fm for modern compounds (Tables S1a,b). For each AA, a 0.1 M liquid standard was prepared in 0.1 M hydrochloric acid (HCl) in Milli-Q water. The DOC concentration of Milli-Q water has been reported to be  $0.9 \pm 0.2 \mu\text{M}$ ,<sup>34</sup> 5 orders of magnitude less than the DOC concentration in our dissolved AA standards. On the basis of this concentration range, the maximum single-peak injection volume for this study (19  $\mu\text{L}$ ) would contain  $2 \times 10^{-4}$   $\mu\text{g}$  of DOC from the Milli-Q system. Therefore, the dissolution of powder standards in Milli-Q is extremely unlikely to represent any appreciable contribution to the blanks we measured for this method. Aliquots of the Ala, Glu, Gly, Met, Thr, and Val liquid standards were combined to make a 6 AA standard containing 1.7  $\mu\text{g}$  of C  $\mu\text{L}^{-1}$  of each AA.

**HPLC System and Compound Isolation.** The HPLC system (Shimadzu Scientific Instruments, Inc., Columbia, MD, USA) was equipped with a system controller (SCL-10A vp), degasser (DGU-20A5), two pumps (LC-20AD), and autosampler with an adjustable injection volume of 0.1–100  $\mu\text{L}$  (SIL-20A). A mixed media column (SiELC Primesep A, 10  $\times$  250 mm, 100  $\text{\AA}$  pore size, 5  $\mu\text{m}$  particle size; SiELC Technologies Ltd., Prospect Heights, IL, USA) was used for compound separation. This is a reversed-phase, semipreparative scale column embedded with strong acidic ion-pairing groups to provide additional retention mechanisms for compounds with mixed functionality, such as AAs. An adjustable flow splitter (Analytical Sales and Services, Inc., Pompton Plains, NJ, USA) was used inline following the chromatography column to direct approximately 7% of the flow to an evaporative light scattering detector (ELSD-LT II, Sedex 85LT; SEDERE, Alfortville, France) for compound detection. The remaining eluent was directed to a Shimadzu time-based automated fraction collector (FRC-20A).

The AA standards were injected in a size series containing 0, 10, 50, and 85  $\mu\text{g C/AA}$ . Compounds were separated using a binary solvent gradient program adapted from a recently

published method for maximal separation of protein AAs developed for this particular column (Figure 2).<sup>28</sup> The mobile

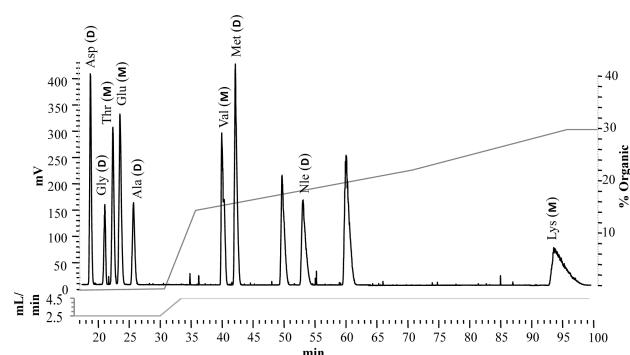


**Figure 2.** Representative sample chromatogram under typical conditions used to collect individual AAs for  $^{14}\text{C}$  measurements. Solid line and secondary axis indicate solvent gradient (organic phase: 0.1% TFA in acetonitrile; aqueous phase: 0.1% TFA in water). The flow rate is shown below the chromatogram. AA abbreviations are as defined in the text. D and M indicate AAs with either dead or modern  $^{14}\text{C}$  Fm values.

phase consisted of 0.1% (v/v) trifluoroacetic acid (TFA) in Milli-Q water (aqueous phase) and 0.1% (v/v) TFA in acetonitrile (organic phase). The solvent ramp program was as follows: Starting with 100% aqueous/0% organic with a total flow rate of 2.5 mL/min, ramp to 0.5% organic from 0 to 30 min; ramp total flow to 4.5 mL/min from 30 to 33.5 min, increasing from 0.5 to 15% organic from 30 to 35 min. Ramp from 15 to 22.5% organic from 35 to 70 min; ramp from 22.5 to 30% organic from 70 to 95 min, and hold at 30% organic from 95 to 140 min. The column was then cleaned and equilibrated by increasing to 100% organic and holding from 140 to 155 min, decreasing to 50% and holding from 155–160 min, ramping to 0% at 2.5 mL/min from 160 to 165 min, and holding until 170 min. The individual AA peaks were collected in 1–3 precombusted (450  $^{\circ}\text{C}/4$  h) glass vials, depending on eluent volume, using the automated fraction collector.

**Sample Processing, AMS  $^{14}\text{C}$  Measurements, and Blank Calculations.** After fraction collection, the mobile phase was removed using a Jouan centrifugal evaporator (Societe Jouan, Saint-Herblain, France) at a chamber temperature of 55  $^{\circ}\text{C}$ . Dry AA residues were then redissolved into 100–150  $\mu\text{L}$  of 0.1 M HCl, transferred into precombusted quartz tubes, dried, amended with precombusted cupric oxide ( $200 \pm 50$  mg) and silver wire (approximately 1  $\times$  1 mm diameter), and flame-sealed under vacuum.

The  $\text{CO}_2$  generated from each sample was measured manometrically after sealed tube combustion. The samples were then prepared for AMS  $^{14}\text{C}$  measurements using the sealed tube zinc reduction method of graphitization.<sup>32,33</sup> Typically, 8–10 individual AMS measurements were obtained from each target. The Fm values are corrected for mass-dependent fractionation using online AMS  $\delta^{13}\text{C}$  determined values and are reported following the conventions set forth by Stuiver and Polach.<sup>35</sup> Small sample blank corrections were performed using modern and dead AA pairs following the indirect method.<sup>29,36</sup> The uncertainty in the mass of each MC or DC blank is reported as  $\pm 50\%$  of the blank mass itself.



## RESULTS AND DISCUSSION

The indirect method of C blank characterization we used here, employing small standards processed as samples, is preferable to direct determination of C blanks.<sup>37</sup> This is especially true when blanks for a single isolation protocol are expected to be too small to measure directly from a single analytical run, therefore necessitating pooled blanks to collect enough material for a single direct blank measurement. This introduces significant error and also precludes assessment of blank variability.<sup>37</sup> The indirect method of blank quantification using modern-dead process standards accounts for a sample “matrix effect”, whereas direct blank measurements do not, and also provides more accurate estimates of the variability in the blank than the isotope dilution method.<sup>38</sup>

**Quantification of MC and DC Blank Amounts.** MC and DC blank masses, and specifically changes in uncorrected measurement accuracy with decreasing sample size, can first be assessed by plotting the deviation from the known ratio to OX-1 for modern or dead standards against the total sample size. In this approach, the expected deviation from the known isotopic ratio across a range of sample sizes is given by a modern carbon correction (MCC(M), eq 3) to offset a constant-mass MC blank for a size series of <sup>14</sup>C-dead samples or a dead carbon correction (DCC(M), eq 4) to correct for a constant-mass DC blank for <sup>14</sup>C-modern samples. These equations are linear in log–log scale, and for constant blank amounts (*d* and *m*, eqs 3 and 4), they are functions of sample size (M) only. The diagonal lines in Figure 3 a, b each represent a MCC(M) or DCC(M), derived from a constant MC or DC blank amount across sample sizes. When the measured isotopic ratios (without blank correction) are plotted on the same axes, the MC and DC blank masses are indicated by the nearest MCC(M) or DCC(M) lines.

Panels a and b in Figure 3 show that the total procedural blanks follow expected behavior for constant blank additions.<sup>24,30</sup> The MC blanks fall between the lines representing 0.4–2.0  $\mu\text{g}$  of C, and DC blanks fall between 0.7 and 3.0  $\mu\text{g}$  of C. A single outlier (Nle, indicated by \* in Table S1b) falls outside these ranges. This sample was measured early in the method development, suggesting contamination that was not present in any of our subsequent measurements as we refined our techniques. The combined drying, combustion, and graphitization blanks fell between the 0.7–1.0  $\mu\text{g}$  of C MCC(M) lines and the 0.7–2.0  $\mu\text{g}$  of C DCC(M) lines, indicating that less than 1.0  $\mu\text{g}$  of MC and 2.0  $\mu\text{g}$  of DC were attributable to post-HPLC processing. These data are consistent with the expectation that more intensive sample preparation protocols introduce larger procedural blanks. The data for each sample set display the expected trend of larger offsets from the known ratio for smaller samples. Despite these trends, the data for each sample set is not always linear within AMS uncertainty (error bars as shown). The uncertainty in the MC or DC blank mass, conservatively reported as 50% of the mass itself, is needed to account for this additional variability.

The graphical approach is a starting point for the calculation of MC and DC blank masses (eq 5). In this calculation,<sup>29,39</sup> MC and DC blank masses are determined based on their proximity to diagonal lines in Figure 3, and such that all standards in each AA pair are corrected to the known standard Fm within the total propagated uncertainty. The total reported blank masses (Tables S1 and S2) are then the sum of the independently determined MC and DC contributions.

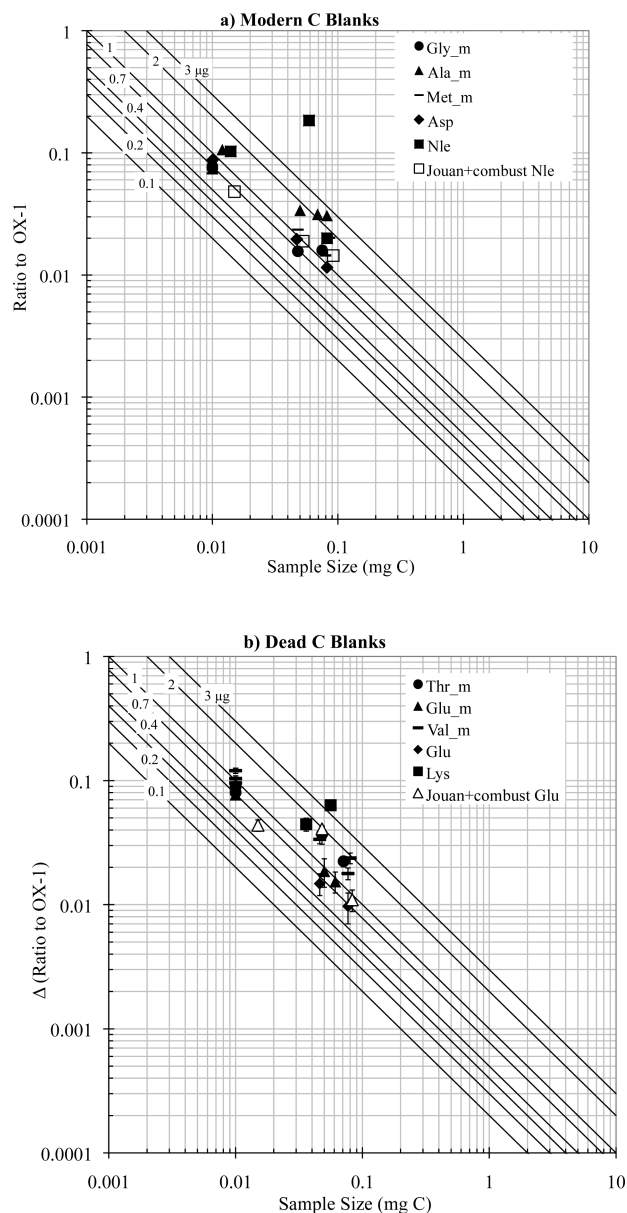


**Figure 3.** Mixing models for blank assessment. (a) The MC blank for the dead AA in each pair and (b) the DC blank for the modern AA in each pair are approximated using two-component mixing models.<sup>29</sup> The diagonal lines represent the expected values for constant blank amounts of 0.1, 0.2, 0.3, 0.4, 0.7, 1, 2, and 3  $\mu\text{g}$  of MC or DC within a given total sample size ( $\mu\text{g}$  of C values indicated at upper left on each diagonal line). The suffix “m” indicates a value was derived from a chromatographically separated AA mixture. MC blank amounts (panel a) are assessed using the increase in the measured ratio to OX-1 as <sup>14</sup>C-dead sample sizes decrease; instrumental errors are smaller than the symbols. DC blanks (Panel b) are determined from the decrease in measured ratio to OX-1 as <sup>14</sup>C-modern sample sizes decrease; error bars represent instrumental uncertainty of  $\pm 1$  SD.

The calculated MC and DC blank masses (Figure 4, Tables S1 and S2) generally correspond well with the blank ranges indicated by the graphical approach (Figure 3a, b). Small discrepancies are likely due to the fact that, unlike eq 5, the plots assume that the known ratio to OX-1 is 1 or 0; however, real “modern” AAs available today have some bomb carbon and are thus slightly “futuristic” ( $R_{\text{spl}} > R_{\text{std}}$ ), whereas those treated as dead actually have a small amount of <sup>14</sup>C ( $R_{\text{spl}} > 0$ ). This

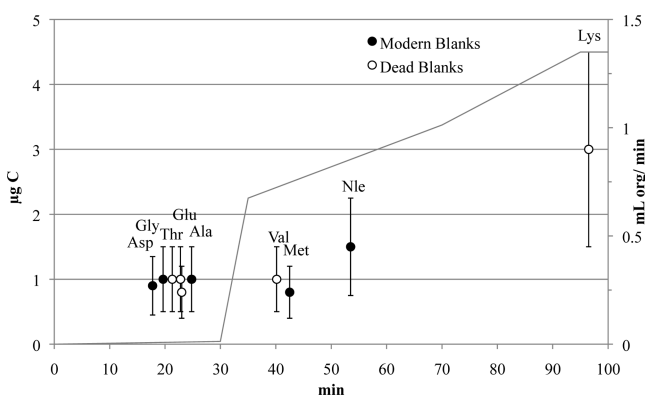


**Figure 4.** Blank size relative to chromatographic retention time. The MC or DC blanks ( $\mu\text{g}$  of C) calculated for each AA standard are shown. Filled circles indicate MC blanks calculated from dead AAs; open circles indicate DC blanks calculated from modern AAs. The solid line is associated with the secondary  $y$ -axis, indicating organic eluent flow rate. Error bars indicate uncertainty in the mass of the blank, reported as  $\pm 50\%$  of the calculated blank mass. Total reported blanks include the MC or DC blank calculated from each AA, as well as the DC or MC blank calculated from its partner.

leads to a higher ratio to OX-1 for dead AAs, indicating larger MC blanks. However, this effect is addressed when MC and DC blank masses are determined by calculation, and consistent corrections across several AA size series bring each within error of its known value.

The calculated total procedural blanks for HPLC-processed AA standards ranged from 0.8 to 1.5  $\mu\text{g}$  of MC and 0.8–3  $\mu\text{g}$  of DC (Figure 4, Table S1). The early eluting AA had smaller blank contributions. The indirect method indicated that  $0.9 \pm 0.45$   $\mu\text{g}$  of MC and  $0.8 \pm 0.4$   $\mu\text{g}$  of DC were incorporated into the Asp/Glu pair (injected individually) and  $1.0 \pm 0.5$   $\mu\text{g}$  each of MC and DC for the Gly/Thr, Glu/Ala, and Val/Met pairs injected within our 6 AA standard mixture. Calculated blanks were somewhat larger for the later eluting AA standards ( $1.5 \pm 0.75$   $\mu\text{g}$  of MC and  $3.0 \pm 1.5$   $\mu\text{g}$  of DC from Nle/Lys, injected individually).

These total blank levels are relatively low in the context of AMS  $^{14}\text{C}$  measurements. For example, Shah and Pearson<sup>22</sup> determined a total blank of approximately 2  $\mu\text{g}$  of C (depending on eluent volume) for their lipid isolation protocol in which compounds elute in ethyl acetate, and Ingalls et al.<sup>11</sup> report total blanks of 2.1  $\mu\text{g}$  of C for the HPLC purification of lignin phenols, where compounds elute in a variable blend of isopropyl alcohol and hexane. Birkholz et al.<sup>30</sup> found a similar blank of 2  $\mu\text{g}$  of C for their HPLC purification of specific membrane lipids, but only after an extra purification step using a normal-phase column to remove contaminants added by the reverse-phase column. Repeta and Aluwihare<sup>40</sup> used pooled, composite blanks to estimate that their HPLC purification of neutral sugars from marine DOM introduced 6–12  $\mu\text{g}$  of total C/peak, and Marom et al.<sup>31</sup> reported a total blank of 3.3  $\mu\text{g}$  of C for their purification of the single AA hydroxyproline based on a method in which water was the only mobile phase. In the context of these prior studies, the blanks calculated for our HPLC method are comparable to the lowest blank levels reported by other chromatography-based CSRA protocols.

**Major Blank C Sources.** The procedural MC and DC blanks could be derived from either HPLC separation or downstream sample processing. Therefore, isolating specific blank sources in the full analytical stream represents a critical

component of method assessment. This information can point to possible ways to further reduce blank sizes for the smallest samples and also allows predictions to be made regarding the possible effects of method modification. As described above, our experimental design (Figure 1) allowed us to individually isolate MC and DC blank contributions from the three major protocol components: HPLC isolation, drying, and combustion/graphitization.

Calculations based on the indirect method indicated corrections of  $0.7 \pm 0.35$   $\mu\text{g}$  of MC and  $0.01 \pm 0.2$   $\mu\text{g}$  of DC for combined combustion/graphitization blanks (Figure S1 and Table S2). The size and modern isotopic composition of this blank is consistent with previously reported combustion blanks.<sup>22</sup> For isolating the effects of sample drying within the protocol, blanks were calculated for samples prepared from liquid standards and compared to the combustion/graphitization blank for powder standards (see Experimental Section). Our results suggest sample drying introduced  $0.1 \pm 0.5$   $\mu\text{g}$  of MC and  $0.8 \pm 0.5$   $\mu\text{g}$  of DC (Table S2). Together, these results indicate that sample drying and combustion blanks accounted for most of the total procedural blank for the early eluting AAs.

The relative HPLC blank sizes varied with retention time (Figure 4), suggesting a relationship between mobile phase volume/composition and exogenous C. Earlier peaks, during the period where the mobile phase was predominantly aqueous, all had the lowest total blanks (2  $\mu\text{g}$  of C), whereas the latest-eluting AA, collected during the highest organic mobile phase composition, had significantly elevated blanks (4.5  $\mu\text{g}$  of C). Column bleed and mobile phase solvents have in the past been found to be the two main contributors to the HPLC C blanks for well-separated peaks.<sup>5,19,22</sup> The larger blanks for late eluting peaks are most likely related to increasing percentages of organic eluent. Increased solvent flow rates and longer peak collection windows due to typical peak broadening would also increase the total volume of organic solvent collected with each peak. In particular, the strong increase in the DC blank for the latest eluting peaks (Nle and Lys; 3  $\mu\text{g}$  of DC) are consistent with these factors, and the hypothesis of column bleed and organic solvent-derived blanks, because these sources should be  $^{14}\text{C}$ -depleted. For example, Repeta and Aluwihare<sup>40</sup> directly measured an LC blank at  $-700$  to  $-800\%$  using the same solvent system (acetonitrile and water), and evidence by McCullagh et al.<sup>19</sup> strongly suggests that column bleed from the Primesep A column is  $^{14}\text{C}$ -dead.

Although the marked increase in HPLC DC blanks for the late-eluting AAs Nle and Lys is consistent with expected DC sources, the MC blank also increases somewhat for this same late-eluting pair (1.5  $\mu\text{g}$  of MC). This result is most likely a correction bias we introduce by applying the same correction to Nle and Lys, which have very different RTs and eluent volumes (Nle: RT = 51–56 min, 19 mL of eluent; Lys: RT = 90–103 min, 58.5 mL of eluent). However, using  $^{14}\text{C}$ -modern/dead AA pairs to separately quantify endmember contributions to the total C blank requires paired AAs to have identical blanks. In this case, eluent volume and composition suggest that only a fraction of the large DC blank calculated from the modern AA Lys is actually present in the collected Nle peaks. Calculating the MC blank for this pair would therefore produce an inflated MC blank amount to compensate for the excessive DC blank correction in Nle. Our HPLC-derived blanks suggest primarily DC sources for column and mobile phase material with eluent volume serving as the largest contributor to HPLC blanks.

A final consideration for accurate CSRA of chromatographically purified compounds is the potential influence of adjacent peaks. Adequate separation of adjacent compounds is essential for isotopic analyses, where any error due to partial coelution or peak carry-over can be greatly magnified by intrapeak isotope fractionation as well as isotopic value offsets between adjacent compounds.<sup>27,28</sup> In practice, the potential isotopic effect of any minor coelution or carryover would depend very strongly on the *offset* in Fm values of adjacent compounds. For example, a large coelution of two peaks with similar C isotopic composition would have little effect on the measured Fm values, whereas a small coelution of two peaks with very different Fm values could significantly alter results. In our experimental design, we compare modern to dead adjacent peaks, which is the most sensitive test for isotopic effects due to coelution. Within this design, the comparison of our blank values from the mixed standard to individually injected peaks clearly shows that neighboring peaks, even those with the most limited baseline separation in our method, have no measurable impact on <sup>14</sup>C values (Figure 4). Total blanks for all of the early eluting AAs are in the range of 1 μg of MC and 1 μg of DC, regardless of whether the blank was determined from individual AA injections or the mixed standard.

**Blank Corrections for Small-Sample Amino Acid <sup>14</sup>C Measurements.** The ultimate goal of this method is to allow accurate CSRA of individual AAs. Therefore, it is critical to assess if corrections based on the blanks determined here can produce accurate values and over what range of sample sizes these corrections can be applied. Figure 5 compares measured Fm values of AAs in our mixed standard with those obtained after correction using the blank amounts determined for the corresponding AA pair. Corrections were applied to samples containing a range of 10–86 μg of C. After correction using our procedural blank amounts (Figure 4, Table S1), most values are within error ( $\pm 1$  SD) of the independently measured “known” Fm values. This data also shows that although the smallest samples (10 μg C) were the most affected by the blank correction, even these are corrected within error of the known value by our approach.

For potential environmental applications of CSRA-AA, the uncertainty of corrected values is also a central consideration. Our data shows a significant increase in uncertainty with decreasing sample size (Figure 6). This effect is known to be predominately due to blank C contributions.<sup>29</sup> Uncertainties in MC or DC blank amounts are reported as 50% of the blanks themselves, so larger blanks contribute more uncertainty to the corrected <sup>14</sup>C Fm values. The offset between the early- and late-eluting series in Figure 6 illustrates this effect. The uncertainty of corrected Fm values increases rapidly below 20 μg of C for most AA and at 60 μg of C for the late-eluting series. This suggests that a target sample size of 20 μg of C would yield uncertainty of 1 SD total propagated error less than  $\pm 0.02$  Fm (equivalent to  $\pm 20\%$ ) for most of the protein AAs. However, later eluting peaks (e.g., chromatographic region of Nle and Lys in this method) would require substantially more sample (>60 μg of C) to obtain similar uncertainty.

A major implication of these results is therefore that, for sample-limited materials, target sample size must take into account chromatographic elution order and should be scaled to the uncertainty required. Finally, we note that the uncertainty obtained for the smallest samples tested (10 μg of C) is far lower in all cases (1 SD =  $\pm 0.05$ – $0.07$  Fm, or 51–82 ‰). Thus, researchers should be cognizant of these limitations when

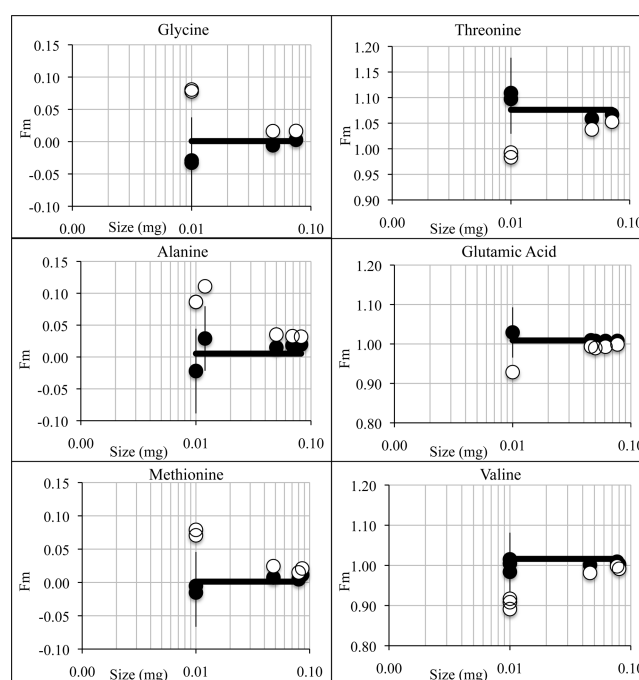


**Figure 5.** Fraction modern results after blank correction. The corrected, uncorrected, and known Fm values for all peak loadings for AA in the mixed standard are shown (uncorrected values: open symbols; corrected values: filled symbols; known values: solid lines). Although modern blanks raise the uncorrected Fm value for the dead standards (and vice versa for modern standards), the corrected Fm values obtained using the blank amounts determined for the method are within error of standard values for all AAs. Each AA pair is corrected individually, e.g., all of the samples from Gly and Thr are corrected together using the blanks calculated from this pair. Error bars for corrected values represent  $\pm 1$  standard deviation for propagated blank and AMS uncertainty. Known values were obtained from large ( $\sim 0.8$  mg) samples without HPLC processing.

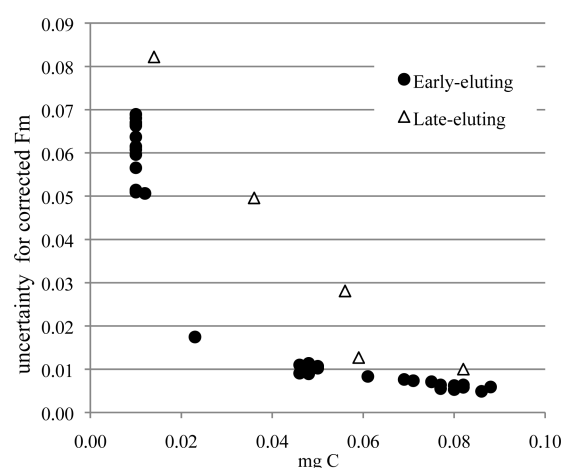


**Figure 6.** Relationship of Fm measurement uncertainty (1SD) to AA sample size. Total propagated uncertainty (AMS, MC, and DC blank mass) for blank-corrected HPLC-processed AA samples increases dramatically for the smallest samples and is also strongly linked to elution order. For early eluting peaks (most AA; closed circles), the method allows uncertainty of  $<0.02$  Fm for samples  $>20$  μg of C. In contrast, late-eluting AA (open triangles; Nle and Lys only) require  $>60$  μg of C for similar uncertainty, owing to greater uncertainty in the elevated blank amounts resulting from higher organic eluent volumes collected with the peaks.



selecting practical sample size lower limits based on their desired application. The necessary level of uncertainty will depend on the range of values found in a given environment or sample set. The 20  $\mu\text{g}$  of C for the  $\pm 20\%$  threshold for most protein AAs by our method is similar to the current threshold for small-sample AMS measurements (e.g., 10  $\mu\text{g}$  of C to  $\pm 1\%$  precision).<sup>24</sup> Our method's sample size requirements and uncertainty are also comparable to other HPLC-based CSRA approaches.<sup>11,22</sup> These results should account for the blanks associated with the entire sampling protocol because the purification of the target molecule inherent to CSRA effectively removes other forms of exogenous C introduced upstream.

## CONCLUSIONS

We have quantified both MC and DC blanks, as well as characterized their main analytical sources, for an HPLC method designed to purify a suite of individual protein AAs for CSRA. The total blanks introduced by HPLC purification, sample drying, sample transfers, combustion, and graphitization are in the range of  $1.0 \pm 0.5 \mu\text{g}$  of MC and  $1.0 \pm 0.5 \mu\text{g}$  of DC for AAs that elute relatively early in the chromatography program. These blank masses are within error of those calculated for the downstream processing steps, indicating that the low volumes of eluent for these early RT AAs do not introduce appreciable exogenous C. In contrast, for later-eluting AAs, the HPLC separation contributes to an increased DC blank ( $1.5 \pm 0.75 \mu\text{g}$  of MC and  $3.0 \pm 1.5 \mu\text{g}$  of DC) attributable mainly to the increased eluent volume. Corrected values for the HPLC-processed samples are consistently within error of the known values, although the uncertainty increases for small ( $<10 \mu\text{g}$  of C) samples. The sample size required for a given uncertainty is also strongly linked to eluent volume and composition with uncertainty becoming progressively higher for the later-eluting AAs. To our knowledge, the linkages between elution order,  $^{14}\text{C}$  blanks, and sample size requirements has not been explicitly quantified previously, but likely represents an important consideration for any HPLC-based CSRA protocol employing binary solvent gradients.

Our study has verified the potential of a simple, single-column HPLC method to produce accurate  $^{14}\text{C}$  Fm values for a suite of protein AAs, with environmentally meaningful uncertainty, and at sample sizes approaching the current cutting-edge threshold of AMS measurements. Although a few prior studies have reported individual AA  $^{14}\text{C}$  values, to our knowledge, this work represents the first rigorous quantification of C blank amounts and sources for any CSRA-AA protocol. Sample size requirements for accurate  $^{14}\text{C}$  analyses are largely determined by the size of process blanks. Our method decreases sample size requirements more than 10-fold relative to earlier methods.<sup>19</sup> The far greater number of isolable AAs in our method broadens its potential applications. AAs are the primary organic N form in most detrital organic N pools on Earth, including dissolved organics in natural waters, humic N in soils, and sedimentary organic N.<sup>13</sup> Our results suggest that CSRA-AA can be used as a powerful tool for understanding the N cycle. For example, many AAs originate from primary production and others from bacterial diagenesis.<sup>15,41,42</sup> One potential application of CSRA-AA could be to understand microbial alteration of labile organic C and N cycling. Because the low sample size requirements of this method are compatible with AA amounts that can be isolated from most natural sample types, and the method uncertainty is low, it could be widely

applied to elucidate cycling and preservation of organic N across many environments.

Future work should likely focus on understanding differences in  $^{14}\text{C}$  AA content of individual AAs and specifically how well our current method can measure key tracer AA in environmental contexts. One particularly useful area of future applications may be to understand oceanic N cycling. The  $\pm 20\%$  uncertainty achieved for AA samples of 20  $\mu\text{g}$  of C can easily distinguish between deep-ocean dissolved inorganic C, particulate organic C, and high and low molecular weight dissolved organic C,<sup>43,44</sup> suggesting this new tool can be used to investigate microbial metabolism in the deep ocean. Our method's uncertainty should allow for differentiating the cycling of marine dissolved organic matter biochemical fractions,<sup>43</sup> dynamic coastal upwelling systems with variable organic matter  $\Delta^{14}\text{C}$  source signatures and cycling rates,<sup>45</sup> or organic matter within deep-sea hydrothermal vent systems.<sup>46</sup> We suggest this new method will open up investigations in many previously untenable sample types.

## ASSOCIATED CONTENT

### Supporting Information

The Supporting Information is available free of charge on the ACS Publications website at DOI: 10.1021/acs.analchem.5b03619.

Derivation of the formulas used for blank determination and correction, tabulated data, and a graphical representation of the effects of blank corrections on combusted samples (PDF)

## AUTHOR INFORMATION

### Corresponding Authors

\*Phone 408-410-6764. E-mail: [abour@ucsc.edu](mailto:abour@ucsc.edu).

\*Phone 831-459-1533. E-mail: [mdmccar@ucsc.edu](mailto:mdmccar@ucsc.edu).

### Notes

The authors declare no competing financial interest.

## ACKNOWLEDGMENTS

We gratefully acknowledge Drs. Ellen Druffel, John Southon, and Guaciara dos Santos for their advice, insightful discussions, and comments on an earlier version of this paper. Christopher Glynn (UCI) and Dr. Elizabeth Gier (UCSC) assisted with instrumentation and sample preparation. We also thank an anonymous reviewer for their thoughtful comments, which greatly improved this paper. This research was supported by NSF grant OCE-1358041 to M.D.M., a Keck Carbon Cycle AMS Laboratory Postdoctoral Scholarship to B.D.W., the Packard Foundation for Ocean Science and Technology, and the UCSC Committee on Research.

## REFERENCES

- (1) Nelson, D. E.; Korteling, R. G.; Stott, W. R. *Science* **1977**, *198*, 507–508.
- (2) Mollenhauer, G.; Rethemeyer, J. *IOP Conf. Ser.: Earth Environ. Sci.* **2009**, *5*, 012006.
- (3) Eglinton, T. I.; Aluwihare, L. I.; Bauer, J. E.; Druffel, E. R. M.; McNichol, A. P. *Anal. Chem.* **1996**, *68*, 904–912.
- (4) Ingalls, A. E.; Pearson, A. *Oceanography* **2005**, *18*, 18–31.
- (5) Ingalls, A. E.; Shah, S. R.; Hansman, R. L.; Aluwihare, L. I.; Santos, G. M.; Druffel, E. R. M.; Pearson, A. *Proc. Natl. Acad. Sci. U. S. A.* **2006**, *103*, 6442–6447.
- (6) Kramer, C.; Gleixner, G. *Soil Biol. Biochem.* **2006**, *38*, 3267–3278.

- (7) Cowie, B. R.; Greenberg, B. M.; Slater, G. F. *Environ. Sci. Technol.* **2010**, *44*, 2322–2327.
- (8) Cherrier, J.; Bauer, J. E.; Druffel, E. R. M.; Coffin, R. B.; Chanton, J. P. *Limnol. Oceanogr.* **1999**, *44*, 730–736.
- (9) Hansman, R. L.; Griffin, S.; Watson, J. T.; Druffel, E. R. M.; Ingalls, A. E.; Pearson, A.; Aluwihare, L. I. *Proc. Natl. Acad. Sci. U. S. A.* **2009**, *106*, 6513–6518.
- (10) Ohkouchi, N.; Eglinton, T. I.; Keigwin, L. D.; Hayes, J. M. *Science* **2002**, *298*, 1224–1227.
- (11) Ingalls, A. E.; Ellis, E. E.; Santos, G. M.; McDuffee, K. E.; Truxal, L.; Keil, R. G.; Druffel, E. R. M. *Anal. Chem.* **2010**, *82*, 8931–8938.
- (12) McNichol, A. P.; Ertel, J. R.; Eglinton, T. I. *Radiocarbon* **2000**, *42*, 219–227.
- (13) Cowie, G. L.; Hedges, J. I. *Nature* **1994**, *369*, 304–307.
- (14) McClelland, J. W.; Montoya, J. P. *Ecology* **2002**, *83*, 2173–2180.
- (15) McCarthy, M. D.; Hedges, J. I.; Benner, R. *Science* **1998**, *281*, 231–234.
- (16) McCarthy, M. D.; Benner, R.; Lee, C.; Hedges, J. I.; Fogel, M. L. *Mar. Chem.* **2004**, *92*, 123–134.
- (17) McCarthy, M. D.; Benner, R.; Lee, C.; Fogel, M. L. *Geochim. Cosmochim. Acta* **2007**, *71*, 4727–4744.
- (18) Yamashita, Y.; Tanoue, E. *Mar. Chem.* **2003**, *82*, 145–160.
- (19) McCullagh, J. S. O.; Marom, A.; Hedges, R. E. M. *Radiocarbon* **2010**, *52*, 620–634.
- (20) Marom, A.; McCullagh, J. S. O.; Higham, T. F. G.; Hedges, R. E. M. *Radiocarbon* **2013**, *55*, 698–708.
- (21) Pearson, A.; McNichol, A. P.; Benitez-Nelson, B. C.; Hayes, J. M.; Eglinton, T. I. *Geochim. Cosmochim. Acta* **2001**, *65*, 3123–3137.
- (22) Shah, S.; Pearson, A. *Radiocarbon* **2007**, *49*, 69–82.
- (23) Zhang, X. Y.; Zhao, L.; Wang, Y. X.; Xu, Y. P.; Zhou, L. P. *J. Sep. Sci.* **2013**, *36*, 2136–2144.
- (24) Santos, G. M.; Southon, J. R.; Drenzek, N. J.; Ziolkowski, L. A.; Druffel, E. R. M.; Xu, X. M.; Zhang, D. C.; Trumbore, S. E.; Eglinton, T. I.; Hughen, K. A. *Radiocarbon* **2010**, *52*, 1322–1335.
- (25) Qu, J.; Wang, Y. M.; Luo, G.; Wu, Z. P.; Yang, C. D. *Anal. Chem.* **2002**, *74*, 2034–2040.
- (26) Liu, D. L.; Beegle, L. W.; Kanik, I. *Astrobiology* **2008**, *8*, 229–241.
- (27) Broek, T. A. B.; Walker, B. D.; Andreasen, D. H.; McCarthy, M. D. *Rapid Commun. Mass Spectrom.* **2013**, *27*, 2327–2337.
- (28) Broek, T. A. B.; McCarthy, M. D. *Limnol. Oceanogr.: Methods* **2014**, *12*, 840–852.
- (29) Santos, G. M.; Southon, J. R.; Griffin, S.; Beupre, S. R.; Druffel, E. R. M. *Nucl. Instrum. Methods Phys. Res., Sect. B* **2007**, *259*, 293–302.
- (30) Birkholz, A.; Smittenberg, R. H.; Hajdas, I.; Wacker, L.; Bernasconi, S. M. *Org. Geochem.* **2013**, *60*, 9–19.
- (31) Marom, A.; McCullagh, J. S. O.; Higham, T. F. G.; Sinityn, A. A.; Hedges, R. E. M. *Proc. Natl. Acad. Sci. U. S. A.* **2012**, *109*, 6878–6881.
- (32) Xu, X. M.; Trumbore, S. E.; Zheng, S. H.; Southon, J. R.; McDuffee, K. E.; Luttgen, M.; Liu, J. C. *Nucl. Instrum. Methods Phys. Res., Sect. B* **2007**, *259*, 320–329.
- (33) Xu, X. M.; Gao, P.; Salamanca, E. G. *Radiocarbon* **2013**, *55*, 608–616.
- (34) Griffin, S.; Beupre, S. R.; Druffel, E. R. M. *Radiocarbon* **2010**, *52*, 1224–1229.
- (35) Stuiver, M.; Polach, H. A. *Radiocarbon* **1977**, *19*, 355–363.
- (36) Santos, G. M.; Moore, R. B.; Southon, J. R.; Griffin, S.; Hinger, E.; Zhang, D. *Radiocarbon* **2007**, *49*, 255–269.
- (37) Hwang, J.; Druffel, E. R. M. *Radiocarbon* **2005**, *47*, 75–87.
- (38) Fernandez, A.; Santos, G. M.; Williams, E. K.; Pendergraft, M. A.; Vetter, L.; Rosenheim, B. E. *Anal. Chem.* **2014**, *86*, 12085–12092.
- (39) Mouteva, G. O.; Fahrni, S. M.; Santos, G. M.; Randerson, J. T.; Zhang, Y. L.; Szidat, S.; Czimczik, C. I. *Atmos. Meas. Technol.* **2015**, *8*, 3933–3965.
- (40) Repeta, D. J.; Aluwihare, L. I. *Limnol. Oceanogr.* **2006**, *51*, 1045–1053.
- (41) Calleja, M. L.; Batista, F.; Peacock, M.; Kudela, R.; McCarthy, M. D. *Mar. Chem.* **2013**, *149*, 32–44.
- (42) Dauwe, B.; Middelburg, J. J.; Herman, P. M. J.; Heip, C. H. R. *Limnol. Oceanogr.* **1999**, *44*, 1809–1814.
- (43) Loh, A. N.; Bauer, J. E.; Druffel, E. R. M. *Nature* **2004**, *430*, 877–881.
- (44) Benner, R.; Amon, R. M. W. *Annu. Rev. Mar. Sci.* **2015**, *7*, 185–205.
- (45) Walker, B. D.; Beupre, S. R.; Walker, B. D.; Voparil, I.; Guilderson, T. P.; Druffel, E. R. M. *Geochim. Cosmochim. Acta* **2014**, *126*, 1–17.
- (46) McCarthy, M. D.; Beupre, S. R.; Walker, B. D.; Voparil, I.; Guilderson, T. P.; Druffel, E. R. M. *Nat. Geosci.* **2011**, *4*, 32–36.